AIP | Conference Proceedings

Evaluation of temperature-strain rate dependent uniaxial and planar elongational viscosities for branched LDPE polymer melt

Martin Zatloukal

Citation: AIP Conf. Proc. **1526**, 184 (2013); doi: 10.1063/1.4802613
View online: http://dx.doi.org/10.1063/1.4802613
View Table of Contents: http://proceedings.aip.org/dbt/dbt.jsp?KEY=APCPCS&Volume=1526&Issue=1
Published by the AIP Publishing LLC.

Evaluation of Temperature-strain rate Dependent Uniaxial and Planar Elongational Viscosities for Branched LDPE Polymer Melt

Martin Zatloukal[a,b]

[a]*Polymer Centre, Faculty of Technology, Tomas Bata University in Zlin, nam. T. G. Masaryka 275, 762 72 Zlin, Czech Republic*
[b]*Centre of Polymer Systems, University Institute, Tomas Bata University in Zlin, Nad Ovcirnou 3685, 760 01 Zlin, Czech Republic*

Abstract. In this work, novel rectangle and circular orifice dies have been utilized for temperature-strain rate dependent planar and uniaxial elongational viscosity measurements for the LDPE polymer melt by using standard twin bore capillary rheometer and Cogswell model and the capability of three different constitutive equations (novel generalized Newtonian model, modified White-Metzner model, modified Leonov model) to describe the measured experimental data has been tested. It has been shown that chain branching causes the strain hardening occurrence in both, unixial and planar elongational viscosities and its maximum is shifted to the higher strain rates if the temperature is increased. The level of uniaxial elongational strain hardening for the branched LDPE sample has been found to be higher in comparison with the planar elongational viscosity within wide range of temperatures.

Keywords: Orifice die, Planar elongational viscosity, Uniaxial elongational viscosity, Cogswell model, Entrance pressure drop, Polymer melts, Capillary rheometer, Constitutive equations.
PACS: 47.50.Ef, 83.50.Ha, 83.50.Jf, 83.60.Df, 83.80.Sg, 83.85.Cg, 83.85.Rx

INTRODUCTION

The elongational viscosity represents key rheological parameter allowing understanding the molecular structure of the polymers as well as polymer processing at which the polymer melts are stretched [1-16]. Due to the fact that generation and control of the extensional flow is difficult, experimental determination of the elongational viscosity is a problem [17-20]. Probably the most challenging rheological task is experimental determination of planar elongational viscosity as one can see from very small numbers of experimental data available in the open literature [1-2, 12-16, 21]. With the aim to understand this important rheological parameter in more detail, in this work, novel rectangle and circular orifice dies have been utilized for planar and uniaxial elongational viscosity measurements for branched LDPE by using standard twin bore capillary rheometer and Cogswell model [6, 12] and the capability of three different constitutive equations [22-26] to describe the measured experimental data has been tested.

Novel Trends in Rheology V
AIP Conf. Proc. 1526, 184-193 (2013); doi: 10.1063/1.4802613

EXPERIMENTAL

Extrusion coating, branched LDPE CA820 (Borealis Polyolefine) together with Rosand RH7-2 twin bore capillary rheometer have been utilized for the experimental determination of uniaxial and planar elongational viscosities by using long dies as well as novel orifice dies, which are depicted in Figure 1.

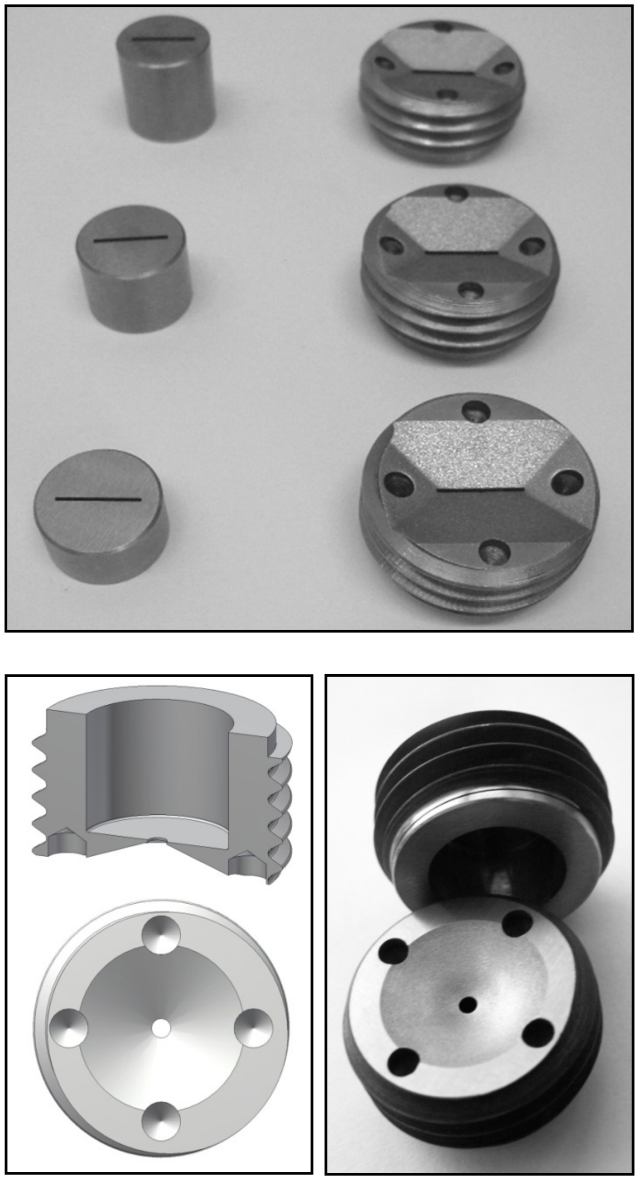

FIGURE 1. Capillary dies with abrupt entry utilized in this work. Top: Set of rectangle dies (CZ UV 23619) for planar elongational viscosity measurements developed in [27] (left – long die, right – orifice die). Bottom: Circular orifice die (CZ UV 19221) for uniaxial elongational viscosity measurements developed in [11].

The main advantage of both utilized orifice dies is the open downstream region design which eliminates any possibility for artificial pressure increase due to polymer melt touching the downstream wall. The uniaxial and planar elongational viscosities have been determined through entrance pressure drop measurements by using the Cogswell model [6, 12] (see Table 1).

Table 1. Cogswell model summarization for uniaxial/planar extensional viscosity determination [6, 12].

	Uniaxial extensional flow	**Planar extensional flow**
Apparent shear rate	$\dot{\gamma}_{\mathrm{app,U}} = \dfrac{4Q}{\pi R^3}$	$\dot{\gamma}_{\mathrm{app,P}} = \dfrac{6Q}{wh^2}$
Corrected shear stress	$\tau_{\mathrm{xy,corr,U}} = \dfrac{\left(P_{\mathrm{L,U}} - P_{0,\mathrm{U}}\right)R}{2L_{\mathrm{U}}}$	$\tau_{\mathrm{xy,corr,P}} = \dfrac{\left(P_{\mathrm{L,P}} - P_{0,\mathrm{P}}\right)h}{2L_{\mathrm{P}}}$
Apparent index of non-Newtonian behaviour	$n_{\mathrm{U}} = \dfrac{d\log\left(\tau_{\mathrm{xy,corr,U}}\right)}{d\log\left(\dot{\gamma}_{\mathrm{app,U}}\right)}$	$n_{\mathrm{P}} = \dfrac{d\log\left(\tau_{\mathrm{xy,corr,P}}\right)}{d\log\left(\dot{\gamma}_{\mathrm{app,P}}\right)}$
Extensional stress	$\sigma_{\mathrm{E,U}} = \dfrac{3}{8}\left(n_{\mathrm{U}}+1\right)P_{0,\mathrm{U}}$	$\sigma_{\mathrm{E,P}} = \dfrac{1}{2}\left(n_{\mathrm{P}}+1\right)P_{0,\mathrm{P}}$
Extensional strain rate	$\dot{\varepsilon}_{\mathrm{U}} = \dfrac{4\tau_{\mathrm{xy,corr,U}}\dot{\gamma}_{\mathrm{app,\,U}}}{3(n+1)P_{0,\mathrm{U}}}$	$\dot{\varepsilon}_{\mathrm{U}} = \dfrac{2\tau_{\mathrm{xy,corr,P}}\dot{\gamma}_{\mathrm{app,\,P}}}{3(n+1)P_{0,\mathrm{P}}}$
Extensional viscosity	$\eta_{\mathrm{E,U}} = \dfrac{\sigma_{\mathrm{E,U}}}{\dot{\varepsilon}_{\mathrm{U}}}$	$\eta_{\mathrm{E,P}} = \dfrac{\sigma_{\mathrm{E,P}}}{\dot{\varepsilon}_{\mathrm{P}}}$

In this table, $P_{0,\mathrm{U}}$ and $P_{0,\mathrm{P}}$ represents the entrance pressure drop measured on annular and rectangular orifice die, respectively, Q is the volume flow rate, R is the capillary die radius, w and h is the width and the gap size of the rectangle die, respectively, $P_{\mathrm{L,U}}$ and $P_{\mathrm{L,P}}$ represents the pressure drop through a long die having circular and rectangular shape, respectively, $P_{0,\mathrm{U}}$ and $P_{0,\mathrm{P}}$ is the orifice pressure drop having circular and rectangular shape, respectively, L is the length of the long die. It should be mentioned that the long die has $L/(2R) = 16$ (or $L/h = 16$) whereas the orifice die has $L/(2R) = 0.1208$ (or $L/h = 0.1208$) as suggested in [10].

THEORETICAL

Generalized Newtonian Fluid Model

In this work, recently proposed generalized Newtonian fluid model has been utilized [22-23]:

$$\tau = 2\eta\left(I_{|\mathrm{D}|}, II_{\mathrm{D}}, III_{\mathrm{D}}\right)D \tag{1}$$

where τ means the extra stress tensor, D represents the deformation rate tensor and η stands for the viscosity, which is not constant (as in the case of standard Newtonian law), but it is allowed to vary with the first invariant of the absolute value of deformation rate tensor $I_{|D|} = tr(|D|)$, (where $|D|$ is defined as the square root of D^2) as well as on the second $II_D = 2tr(D^2)$, and third, $III_D = det(D)$, invariants of D according to Eq. 2

$$\eta(I_{|D|}, II_D, III_D) = A^{1-f(I_{|D|}, II_D, III_D)} \eta(II_D)^{f(I_{|D|}, II_D, III_D)} \tag{2}$$

where $\eta(II_D)$ is given by the well known Carreau-Yasuda model, Eq. 3 and $f(I_{|D|}, II_D, III_D)$ is given by Eq. 4

$$\eta(II_D) = \frac{\eta_0 a_T}{\left[1 + \left(\lambda a_T \sqrt{II_D}\right)^a\right]^{\left(\frac{1-n}{a}\right)}} \tag{3}$$

$$f(I_{|D|}, II_D, III_D) = \left\{ tanh\left[\alpha a_T \left(1 + \frac{1}{4(\sqrt{3})^3}\right)^{-\psi} \left(\left|1 + \frac{III_D}{II_D^{3/2}}\right|\right)^{\psi} \frac{\sqrt[3]{4|III_D|} + I_{|D|}}{3} + \beta \right] \frac{1}{tanh(\beta)} \right\}^{\zeta} \tag{4}$$

here A, η_0, λ, a, n, α, ψ, β, ζ are adjustable parameters and a_T is temperature shift factor defined by the Arrhenius equation:

$$a_T = exp\left[\frac{E_a}{R}\left(\frac{1}{273.15 + T} - \frac{1}{273.15 + T_r}\right)\right] \tag{5}$$

where E_a is the activation energy, R is the universal gas constant, T_r is the reference temperature and T is local temperature.

Modified White–Metzner Model

Modified White-Metzner model constitutive equation is a simple Maxwell model for which the viscosity and relaxation time are allowed to vary with the second invariant of the strain rate deformation tensor [24]. It takes the following form:

$$\tau + \lambda(II_D)\overset{\nabla}{\tau} = 2\eta(II_D)D \tag{6}$$

where $\overset{\nabla}{\tau}$ is the upper convected time derivative of stress tensor, D is the deformation rate tensor, II_D is the second invariant of the rate of deformation tensor, $\lambda(II_D)$ stands for the deformation rate-dependent relaxation time and $\eta(II_D)$ is the deformation rate-dependent viscosity. Although this modification improves the behaviour in steady shear flows, in elongational flows the model predicts unrealistic infinite elongational viscosity. This problem was overcome by Barnes and Roberts [24], who showed that, for specific functions of $\lambda(II_D)$ and $\eta(II_D)$ with $(\lambda_0/K_2) < (\sqrt{3}/2)$ (see Eqs. (3) and (7)), the model does not predict infinite elongational viscosity and can be used for a very good description of elongational viscosity of a wide range of real polymer melts:

$$\lambda(II_{\mathrm{D}}) = \frac{\lambda_0 a_{\mathrm{T}}}{1 + K_2 a_{\mathrm{T}}\, II_{\mathrm{D}}} \tag{7}$$

where λ_0 and K_2 are constants. Eqs. (3, 6-7) together with the physical constraint for λ_0 and K_2 mentioned above represent the modified White–Metzner model.

Modified Leonov Model

This constitutive equation is based on heuristic thermodynamic arguments resulting from the theory of rubber elasticity [25, 28-29]. Mathematically it is relating the stress and elastic strain stored in the material as:

$$\tau = 2\left(c\frac{\partial W}{\partial I_1} - c^{-1}\frac{\partial W}{\partial I_2} \right) \tag{8}$$

where τ is the stress, and W, the elastic potential, depends on the invariants I_1 and I_2 of the recoverable Finger tensor c,

$$W = \frac{3G}{2(n_0+1)}\left\{ (1-\beta)\left[\left(\frac{I_1}{3}\right)^{n_0+1} - 1 \right] + \beta\left[\left(\frac{I_2}{3}\right)^{n_0+1} - 1 \right] \right\} \tag{9}$$

where G denotes linear Hookean elastic modulus, β and n_0 are numerical parameters. Leonov assumed that dissipative process act to produce irreversible rate of strain e_{p}

$$e_p = b\left[c - \left(\frac{I_1}{3}\right)\delta \right] - b\left[c^{-1} - \left(\frac{I_2}{3}\right)\delta \right] \tag{10}$$

which spontaneously reduces the rate of elastic strain accumulation. Here, δ is the unit tensor and b stands for dissipation function defined by Eq. (12).This elastic strain c is related to the deformation rate tensor D as follows

$$\overset{0}{c} - c\cdot D - D\cdot c + 2c\cdot e_p = 0 \tag{11}$$

where $\overset{0}{c}$ is the Jaumann (corotational) time derivative of the recoverable Finger strain tensor. In this work, the neo-Hookean potential (i.e. $\beta = n_0 = 0$ in Eq. 9) and the dissipation function b proposed in [26] (see Eq. 12), have been employed.

$$b(I_1) = \frac{1}{4\lambda}\left\{exp\left(-\xi\sqrt{I_1 - 3}\right) + \frac{sinh\left[\nu\left(I_1 - 3\right)\right]}{\nu\left(I_1 - 3\right) + 1}\right\} \tag{12}$$

Here, ξ and ν are adjustable parameters which are allowed to wary with relaxation time, λ.

RESULTS AND DISCUSSION

The measured temperature-strain rate dependent uniaxial and planar elongational viscosities, together with the shear viscosity and model predictions (model parameters are summarized in Tables 2-4), for the tested branched LDPE sample are provided in Figures 2-5.

TABLE 2. Generalized Newtonian model parameters for T = 170°C (A_1=2.4.10^{-5} Pa, ψ = 8)

η_0 (Pa·s)	λ (s)	a (-)	n (-)	α (s)	β (-)	ζ (-)
4376.6	0.2151	0.4919	0.3464	0.051671	0.0675	0.056076

TABLE 3. Modified White-Metzner model parameters for T = 170°C

η_0 (Pa·s)	λ (s)	a (-)	n (-)	λ_0 (s)	K_2 (s)
4376.6	0.2151	0.4919	0.3464	0.936	1.1286

TABLE 4. Modified Leonov model parameters for T = 170°C

	Maxwell parameters		mLeonov model	
i	λ_i **(s)**	G_i **(Pa)**	ξ	ν
1	10^{-4}	200000.00	0	1.0
2	10^{-3}	94678.18	0	1.0
3	10^{-2}	33507.164	1.7	0.06
4	10^{-1}	12114.745	0.530	0.02
5	1	1329.345	0.14	0.02
6	10	119.607	0	1.0

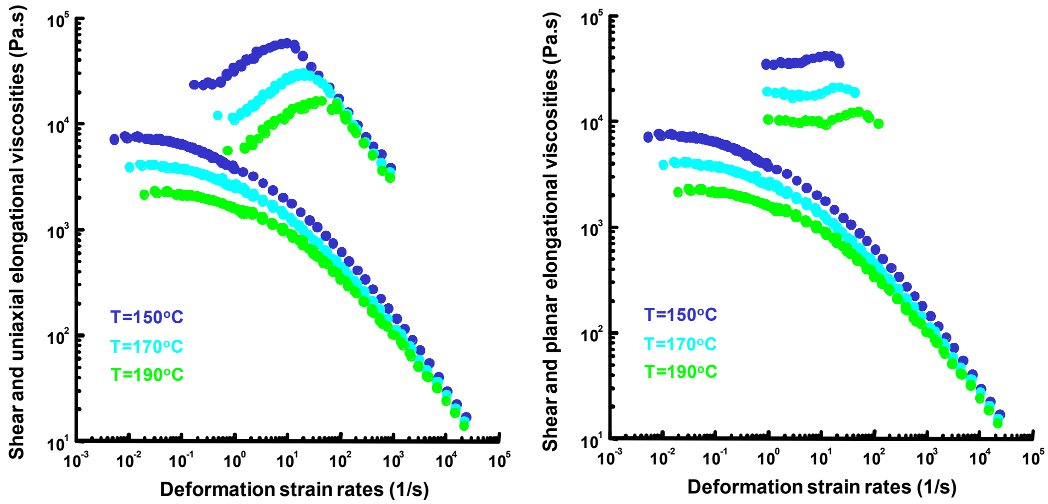

FIGURE 2. Experimentally determined steady shear and elongational viscosities for LDPE sample at three different temperatures. Left: Uniaxial elongational viscosity. Right: Planar elongational viscosity.

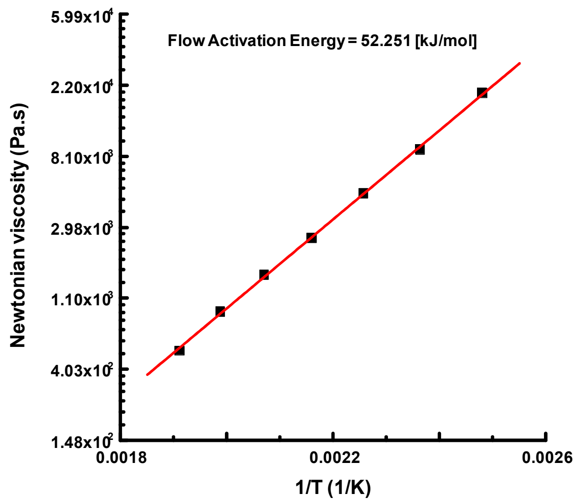

FIGURE 3. Arrhenius plot for LDPE sample.

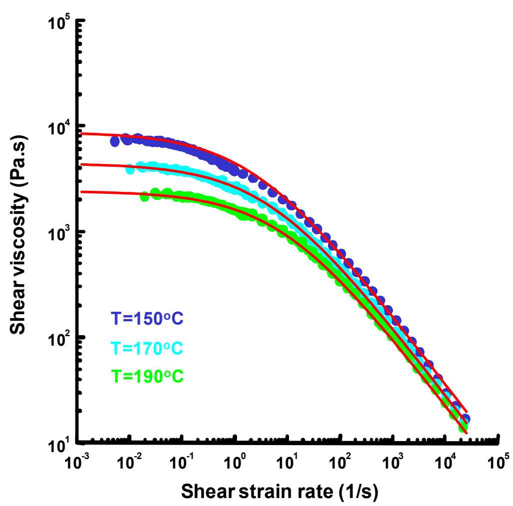

FIGURE 4. Comparison between the utilized generalized Newtonian/modified White-Metzner model fits (solid lines) and measured steady shear viscosities (symbols) for LDPE sample.

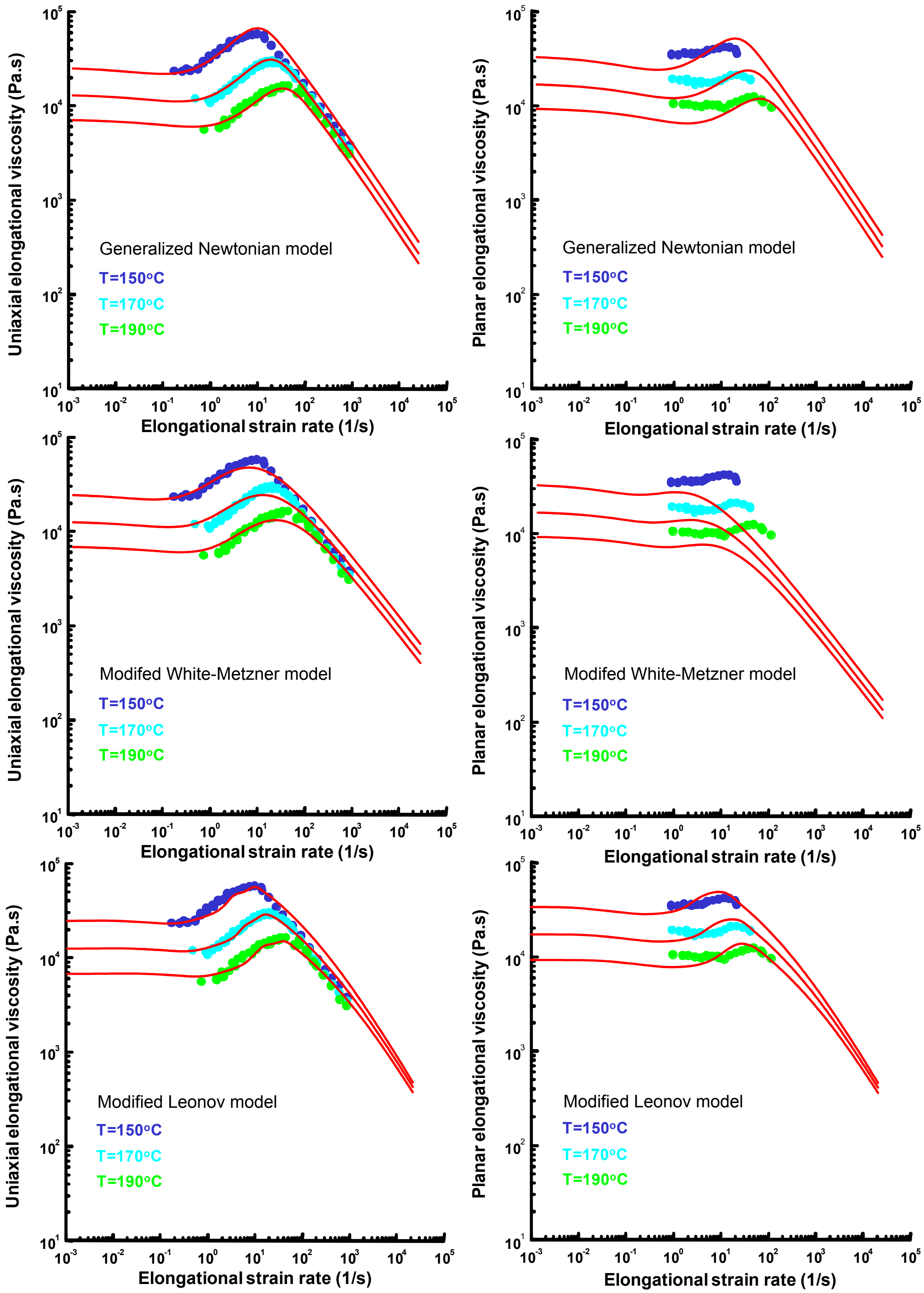

FIGURE 5. Comparison between the utilized model fits/predictions (solid lines) and measured uniaxial and planar elongational viscosities (symbols) for LDPE sample at three different temperatures. Top: Generalized Newtonian model. Middle: Modified White-Metzner model. Bottom: Modified Leonov model.

First, the level of the strain hardening in uniaxial elongational viscosity is higher than in the planar elongational viscosity for the tested LDPE sample at all three temperatures (see Figure 2) which is in good agreement with the recent experimental work performed by D. Auhl et. al [21] on the cross-slot extensional rheometer. Second, the maximum in both viscosities is shifted to the higher strain rates for increased temperature. Third, the generalized Newtonian model has higher capability to describe temperature-strain rate dependent uniaxial and planar viscosities for both tested samples in comparison with modified White-Metzner model. This can be explained by the presence of additional parameter ψ in the generalized Newtonian model allowing to fit the deformation rate dependent planar elongational viscosity, which is not the case of the modified White-Metzner model. Interestingly, the modified Leonov model predictions, based on linear relaxation spectrum and non-linear parameters ξ, ν identified on the steady uniaxial elongational viscosity only, are in the very good agreement with the measured steady planar elongational viscosity. This supports the physics behind the modified Leonov model as well as reliability of the performed measurements.

CONCLUSION

In this work, planar and uniaxial elongational viscosities for branched LDPE polymer melt has been determined through entrance pressure drop techniques on conventional twin bore capillary rheometer by using novel circular and rectangle orifice dies and the obtained experimental data has been described by three different constitutive equations. It has been showed that chain branching causes the strain hardening occurrence in both, uniaxial and planar elongational viscosities and its maximum is shifted to the higher strain rates if the temperature is increased. The level of uniaxial elongational strain hardening for the branched LDPE sample has been found to be higher in comparison with the planar elongational viscosity within wide range of temperatures. It has been found that recently proposed non-Newtonian fluid model [22-23] can represent steady shear, uniaxial and planar elongational viscosities for branched LDPE reasonably well. On the other hand, the modified White-Metzner model has failed in the prediction of the planar elongational viscosity. Interestingly, the modified Leonov model predictions for the planar elongational viscosities have been revealed to be in very good agreement with the experimental data, which supports physics behind the model and reliability of the performed measurements.

ACKNOWLEDGMENTS

The author wish to acknowledge Grant Agency of the Czech Republic (Grant No. 103/09/2066) for the financial support. This article was written with support of Operational Program Research and Development for Innovations co-funded by the European Regional Development Fund (ERDF) and national budget of Czech Republic, within the framework of project Centre of Polymer Systems (reg. number: CZ.1.05/2.1.00/03.0111). The author also wishes to acknowledge Martin Obadal (Borealis Polyolefine) for donation LDPE CA820, which have been used in this work.

REFERENCES

1. F. A. Morrison, *Understanding Rheology*, New York: Oxford University Press, 2001.
2. C. W. Macosko, *Rheology: Principles, Measurements, and Applications*, New York: Wiley-VCH, 1994.
3. H. Münstedt, *J. Rheol.* **23**, 421-436 (1979).
4. M. L. Sentmanat, *Rheol. Acta* **43**, 657-669 (2004).
5. M. L. Sentmanat, B. N. Wang and G. H. McKinley, *J. Rheol.* **49**, 585-606 (2005).
6. F. N. Cogswell, *Polym. Eng. Sci.* **12**, 64-73 (1972).
7. D. M. Binding, *J. Non-Newtonian Fluid Mech.* **27**, 173-189 (1988).
8. A. G. Gibson, *Composites* **20**, 57-64 (1989).
9. S. Kim and J. M. Dealy, *J. Rheol.* **45**, 1413-1419 (2001).
10. M. Zatloukal, J. Vlcek, C. Tzoganakis and P. Saha, *J. Non-Newtonian Fluid Mech.* **107**, 13-37 (2002).
11. M. Zatloukal and J. Musil, *Polym. Test.* **28**, 843-853 (2009).
12. K. Walczak, M. Gupta, K. A. Koppi, J. Dooley and M. A. Spalding, *Polym. Eng. Sci.* **48**, 223–232 (2008).
13. H. M. Laun and H. Schuch, *J. Rheol.* **33**, 119–175 (1989).
14. M. Kraft, "Untersuchungen zur scherinduzierten rheologischen Anisotropie von verschiedenen Polyethylen- Schmelzen", Ph.D. Thesis, Dissertation ETH Zurich Nr. 11417, 1996.
15. P. Hachmann, "Multiaxiale Dehnung von Polymerschmelzen“, Ph.D. Thesis, Dissertation ETH Zurich Nr. 11890, 1996.
16. J. Meissner, S. E. Stephenson, A. Demarmels and P. Portman, *J. Non-Newtonian Fluid Mech.* **11**, 221–237 (1982).
17. R. J. Andrade and J. M. Maia, *J. Rheol.* **55**, 925-937 (2011).
18. T. I. Burghelea, Z. Stary and H. Münstedt, *J. Non-Newtonian Fluid Mech.* **166**, 1198-1209 (2011).
19. H. K. Rasmussen and O. Hassager, *J. Non-Newtonian Fluid Mech.* **171-172**, 106 (2012).
20. T. I. Burghelea, Z. Stary and H. Münstedt, *J. Non-Newtonian Fluid Mech.* **171-172**, 107-108 (2012).
21. D. Auhl, D. M. Hoyle, D. Hassell, T. D. Lord, O. G. Harlen, M. R. Mackley and T. C. B. McLeish, *J. Rheol.* **55**, 875-900 (2011).
22. M. Zatloukal, *Annual Technical Conference - ANTEC, Conference Proceedings* **1**, 92-96 (2011).
23. M. Zatloukal, *J. Non-Newtonian Fluid Mech.* **165**, 592-595 (2010).
24. H. A. Barnes, G. P. Roberts, *J. Non-Newtonian Fluid Mech.* **44**, 113-126 (1992).
25. A. I. Leonov, *Rheol. Acta*, **15**, 85-98 (1976).
26. M. Zatloukal, *J. Non-Newtonian Fluid Mech.* **113**, 209-227 (2003).
27. M. Zatloukal, *AIP Conference Proceedings* **1375**, 163-170 (2011).
28. M. Simhambhatla and A. I. Leonov, *Rheol. Acta* **34**, 259-273 (1995).
29. A. I. Leonov, "Constitutive Equations for Viscoelastic Fluids: Formulation, Analysis and Comparison with Data" in *Advances In the Flow and Rheology of Non-Newtonian Fluids, Part A*, edited by D. A. Siginer, D. De Kee and R. P. Chhabra, New York: Elsevier, 1999.